Design and analysis of 500 GHz heterostructure barrier varactor quintuplers

Mattias Ingvarson, Arne Øistein Olsen, and Jan Stake
Microwave Electronics Laboratory, Chalmers University of Technology,
SE-412 96 Göteborg, Sweden
E-mail: mattias.ingvarson@ep.chalmers.se

Abstract

We report on the design and analysis of heterostructure barrier varactor (HBV) frequency quintuplers with an output frequency of 500 GHz. The HBV is a symmetric varactor, thus only odd harmonics are generated and no DC bias is required. By incorporating several barriers in the device, the HBV is also capable of handling higher power levels than conventional varactors. This makes the HBV superior to the traditional Schottky varactor for high order frequency multiplier circuits. We present analytical, temperature dependent models, which can be used to calculate parameters such as optimum doping concentration, layer structure, device area and series resistance for HBVs, as well as to predict the performance with respect to conversion efficiencies and output power levels. These parameters are then further optimised by harmonic balance simulations in commercial microwave EDA tools, for which we have developed accurate device models. We investigate the influence of embedding impedance levels for optimum conversion efficiency by means of analytical expressions and harmonic balance simulations. Theoretical calculations predict a maximum diode conversion efficiency for a planar, six-barrier InGaAs HBV of more than 30%, for an input power level of 19 dBm. A waveguide circuit realisation of a 500 GHz HBV quintupler is presented.

1 INTRODUCTION

The heterostructure barrier varactor (HBV) [1] is a symmetric varactor consisting of a high band gap semiconductor (barrier), surrounded by moderately doped modulation layers of a semiconductor with a lower band gap. The barrier prevents electron transport through the structure. See Figure 1. When an external signal is applied to the HBV,

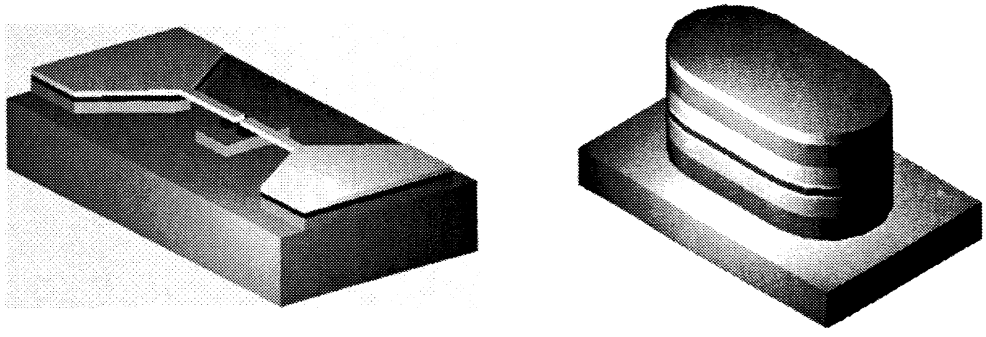

Figure 1 *Schematic views of Chalmers planar HBV diode geometry (left) and a one-barrier HBV mesa (right).*

are accumulated at on side and depleted at the other side of the barrier, causing a symmetric, voltage dependent capacitance. The symmetric C-V and anti-symmetric I-V characteristics of a typical HBV is shown in Figure 2.

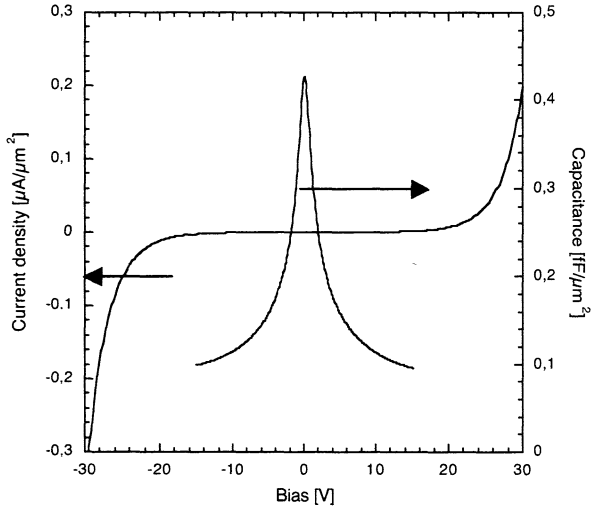

Figure 2. *C-V and I-V characteristics of a typical HBV (CTH-ITME-1819).*

The main advantage with HBVs is the possibility to tailor the layer structure of the device for various applications. The power handling capability can be increased by stacking several barriers epitaxially, or by series connecting mesas. The thickness and doping concentration of the modulation layers have a great influence on the dynamic cut-off frequency, which determines the conversion efficiency.

2 MATERIAL OPTIMISATION

2.1 Material system

HBVs are exclusively fabricated from III-V heterostructures, principally GaAs/AlGaAs on GaAs and InGaAs/InAlAs on InP. GaAs based HBVs exhibit high breakdown voltages but suffer from a low electron mobility and excessive leakage, which lowers the conversion efficiency significantly [2]. State-of-the-art HBVs are fabricated using $In_{0.53}Ga_{0.47}As/In_{0.52}Al_{0.48}As$ on InP [3]. This system offers higher electron velocities and the electron potential barrier is higher compared to GaAs based systems, which means lower leakage currents and, thus, higher conversion efficiencies of frequency multipliers.

2.2 Conversion efficiency

The conversion efficiency of an HBV is closely related to the dynamic cut-off frequency, which therefore needs to be maximised. The dynamic cut-off frequency is defined as

$$f_c = \frac{S_{max} - S_{min}}{2\pi R_s} \tag{1}$$

where S_{max} and S_{min} are the maximum and minimum elastances, respectively, and R_s is the series resistance. The diode conversion efficiency for quintupler operation can be approximated as

$$\eta \approx \frac{100}{1+200\cdot\left(\frac{5}{3}\cdot\frac{f_p}{f_c}\right)^{1.5}}\% \tag{2}$$

where f_p is the pump frequency. For a typical HBV structure, the minimum elastance can be estimated as

$$S_{min} = \frac{N}{A}\left(\frac{b}{\varepsilon_b}+\frac{2s}{\varepsilon_d}+\frac{2L_D}{\varepsilon_d}\right) \tag{3}$$

where L_D is the extrinsic Debye length

$$L_D = \sqrt{\frac{kT\varepsilon_d}{q^2 N_D}}\,. \tag{4}$$

In expressions (3) and (4),

N	number of barriers;
A	device area;
b	barrier thickness;
s	spacer layer thickness;
ε_b	dielectric constant of the barrier material;
ε_d	dielectric constant of the modulation layer;
k	Boltzmann constant;
T	device temperature;
q	elementary charge;
N_D	doping concentration in the modulation layer.

The maximum elastance S_{max} during a pump cycle is determined by the drive level of the HBV, defined as

$$drive = \frac{\max(Q(t))}{Q_{max}} \tag{5}$$

where Q_{max} is the charge at the turn-on voltage, $V_{j,max}$ [4]. Optimum performance is achieved with a maximum elastance swing, low conduction current and drive=1. Under these conditions, the maximum elastance is limited by

$$S_{\max} = \frac{N}{A}\left(\frac{b}{\varepsilon_b} + \frac{2s}{e_d} + \frac{w_{\max}}{\varepsilon_d}\right) \tag{6}$$

where $w_{\max}$ is the maximal extension of the depletion region. For InP based HBVs, $w_{\max}$ is determined by one of the following conditions:

1. depletion layer punch-through, i.e. $w_{\max} = l_D$ where l_D is the thickness of the modulation layers;
2. large electron conduction from impact ionisation at high electric fields;
3. current saturation, i.e. the saturated electron velocity in the material determines the maximum length an electron can travel during a quarter of a pump cycle.

For condition 2, $w_{\max}$ can be calculated as

$$w_{\max} = \frac{\varepsilon_d E_{d.\max}}{qN_D} \tag{7}$$

where $E_{d.\max}$ is the maximum electric field in the modulation layer at break-down. For condition 3, $w_{\max}$ can be estimated as

$$w_{\max} \approx \frac{v_{\max}}{8 f_p}, \tag{8}$$

where $v_{\max}$ is the saturated electron velocity [5].

2.2.1 Series resistance

The series resistance R_s of a planar HBV can be estimated as

$$R_s = R_{active} + 2R_c + 2R_{cl} + R_{spread.buffer} \tag{9}$$

where

R_{active}	resistance of the active layers;
R_c	(ohmic) contact resistance;
R_{cl}	resistance of the contact layers;
$R_{spread.buffer}$	buffer layer spreading resistance.

The mesa resistance is estimated by

$$R_{active} = \frac{(N+2)\cdot l_D}{\mu_D N_D q A} \tag{10}$$

where μ_D is the low field mobility of the modulation layer. The contact resistance is

$$R_c = \frac{r_c}{A} \tag{11}$$

where the specific contact resistance, r_c, depends on the ohmic contact process used, and can be measured by the Transfer Length Method [6]. The resistance of the contact layers is estimated by

$$R_{cl} = \frac{l_{cl}}{\mu_{cl} N_{cl} q A} \tag{12}$$

where l_{cl}, μ_{cl} and N_{cl} are the thickness, low field mobility and doping concentration, respectively, of the contact layers. The buffer layer spreading resistance is the resistance between the two mesas used in the planar geometry, and can be estimated as

$$R_{spread,buffer} = \frac{l_{buff}}{\mu_{buff} N_{buff} q A_{buff}} \tag{13}$$

where l_{buff} and A_{buff} are the equivalent spreading length and area, and μ_{buff} and N_{buff} are the low field mobility and doping concentration, respectively, of the buffer layer between the mesas. l_{buff} and A_{buff} are extracted from FEM simulations performed by FEMLAB.

The low field mobility of the InGaAs contact and modulation layers as a function of doping concentration N and temperature $T$is calculated using the model reported by Sotoodeh *et al.* [7],

$$\mu(N,T) = \mu_{\min} + \frac{\mu_{\max}(300K)(300K/T)^{\theta_1} - \mu_{\min}}{1 + \left(\frac{N}{N_{ref}(300K)(T/300K)^{\theta_2}} \right)^{\lambda}}, \tag{14}$$

where $\mu_{\min}$, $\mu_{\max}$, N_{ref}, λ, θ_1 and θ_2 are fitting parameters available for several III-V compounds.

2.2.2 Optimum doping concentration

By using expressions (3), (6) and (9), the dynamic cut-off frequency can be calculated from (1). Figure 3 shows the cut-off frequency versus doping concentration for an InP HBV structure with 2 to 8 barriers. In order to achieve feasible impedance levels, the area in these calculations is chosen so that

$$\frac{1}{2\pi f_p C_{\max}} = 100. \tag{15}$$

From Figure 3 it can be seen that the optimum doping concentration in the modulation layers is around 10^{23} m^{-3}. However, it should be emphasised that no effect due to self-heating has been considered in the calculations for Figure 3. If too many barriers are stacked epitaxially the device temperature will be very high, which degrades the cut-off frequency [8]. Also, the area for each data point in Figure 3 is chosen according to (15), which means that the area is not constant.

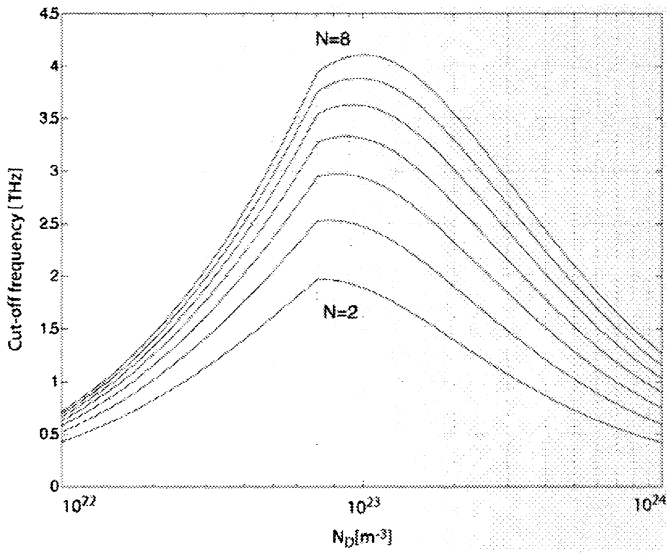

Figure 3 *Cut-off frequency versus modulation layer doping concentration for an InP based HBV material with N=2 to N=8 barriers.*

3 OPTIMUM IMPEDANCE LEVELS

This section investigates optimum embedding impedance levels for 500 GHz HBV quintuplers. First, analytical expressions are used to estimate optimum impedances for a given HBV structure, see e.g. [9]. These impedances are then optimised in Microwave Office, using an in-house HBV model, to predict the performance in terms of conversion efficiency and maximum voltage.

3.1 Harmonic balance simulations

This section presents the results obtained from harmonic balance simulations of HBVs for 500 GHz quintupler applications. All simulations have been carried out using Microwave Office, for which we have developed an accurate HBV diode model. The model is based on the following expression for the voltage across the device versus the charge stored in the HBV [10]:

$$V(Q) = N\left(\frac{bQ}{\varepsilon_b A} + 2\frac{sQ}{\varepsilon_d A} + Sign(Q)\left(\frac{Q^2}{2qN_D\varepsilon_d A^2} + \frac{4kT}{q}\left(1 - e^{-\frac{|Q|}{2L_D AqN_D}}\right)\right)\right) \quad (16)$$

The available input power level around 100 GHz is typically 100 mW or 20 dBm. We assume that the input losses can be limited to 1 dB, and thus the pump power at 100 GHz is set to 19 dBm in all following simulations.

In order to exemplify, we use the fictitious material OPT, optimised for 500 GHz quintupler applications. The material is $In_{0.53}Ga_{0.47}As/In_{0.52}Al_{0.48}As$ on InP. Table I summarises the specifications for the OPT material.

Table I. *Data for the fictitious HBV batch OPT.*

N	b [nm]	s [nm]	l_D [nm]	N_D [m^{-3}]	A [μm^2]	R_s [Ω]	C_{max} [fF]	f_c [THz]
2 x 3	13	5	250	$9.2 \cdot 10^{22}$	37	10.4	13	4.3

3.2 Simulation results

Harmonic balance simulations predict a diode conversion efficiency to 500 GHz of approximately 31% for the OPT HBVs. The device area is chosen to 37 μm^2, in order to assure that the modulation layers are fully depleted when pumped with 19 dBm of input power at 100 GHz. Figure 4 shows the embedding impedances for maximum conversion efficiency for OPT HBVs. The loci of the optimum impedance levels are closely related to the device area. This means that diodes with the same area but different parameters such as doping concentration, material system, number of barriers etc. require very similar embedding impedances for optimum performance.

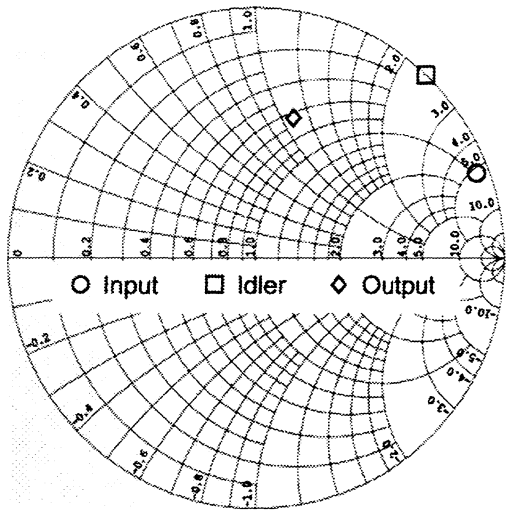

Figure 4. *Optimum embedding impedances for OPT HBVs.*

Figure 5 shows contour plots of the conversion loss for OPT HBVs, obtained from harmonic load pull simulations. The maximum conversion efficiency is 31%, corresponding to a minimum conversion loss of 5.1 dB. Each contour corresponds to an increase in conversion loss of 1 dB. From Figure 5 it is clear that the input matching is very crucial, whilst a non-optimum idler reflection coefficient will not have a very large impact on the circuit performance, as long as the reactance is kept smaller than the optimum value. An accurate impedance match at the input can be achieved by using moveable tuners.

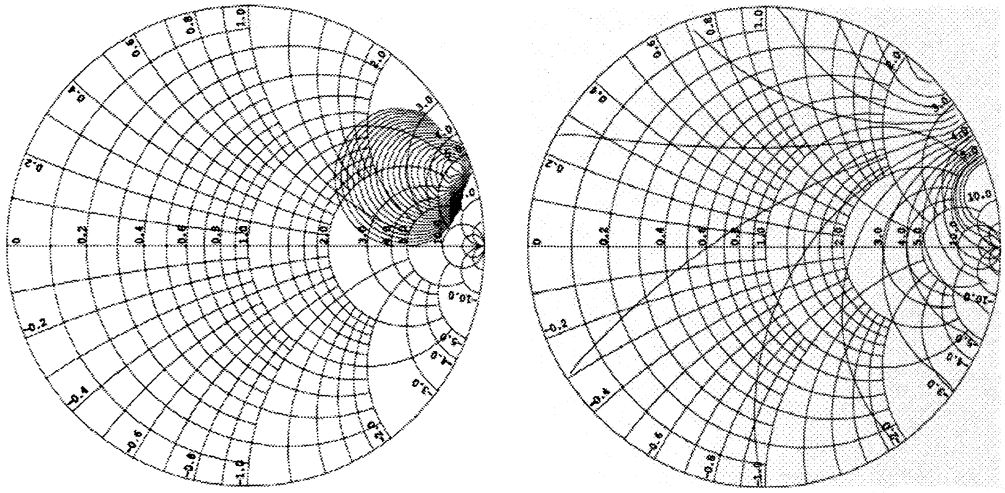

Figure 5. *Conversion loss contours versus (left) input and (right) idler reflection coefficient. The minimum conversion loss is 5.1 dB and the contours correspond to an increase in conversion loss of 1 dB.*

4 WAVEGUIDE CIRCUIT QUINTUPLER REALISATION

Given the relatively high frequency of operation, it is necessary to employ some kind of waveguide structure to realise a 500 GHz HBV quintupler. Figure 6 shows a possible microstrip waveguide circuit realisation, highly suitable for monolithic integration, where the HBV is embedded along with parts of the matching network on a common substrate. This design is based on the HBV tripler design reported by Olsen *et al.* [11]. The fifth and idler impedances are realised using microstrip components, whilst the fundamental frequency is matched using tuners in the input waveguide. It is also possible to use a backshort in the output waveguide to further adjust the embedding impedance levels. However, the aim is that the final version of this circuit shall be fixed tuned at the output. The microstrip circuit is placed in a narrow channel between the input and output waveguides. Beam leads are used to attach the circuit to the waveguide block. A membrane technique with a very thin supporting substrate, e.g. BCB, can be employed to realise this topology. The whole circuit will thus be positioned in air, and the medium will then support a more pure TEM-mode compared to the microstrip mode.

The standard type Archer waveguide has a reduced height across the diode, but this design uses a standard height waveguide. This makes the waveguide block very flexible, as only the microstrip circuit needs to be replaced when different designs are to be tested. A drawback with this approach is that the planar circuit elements exhibit higher losses compared to traditional waveguide elements.

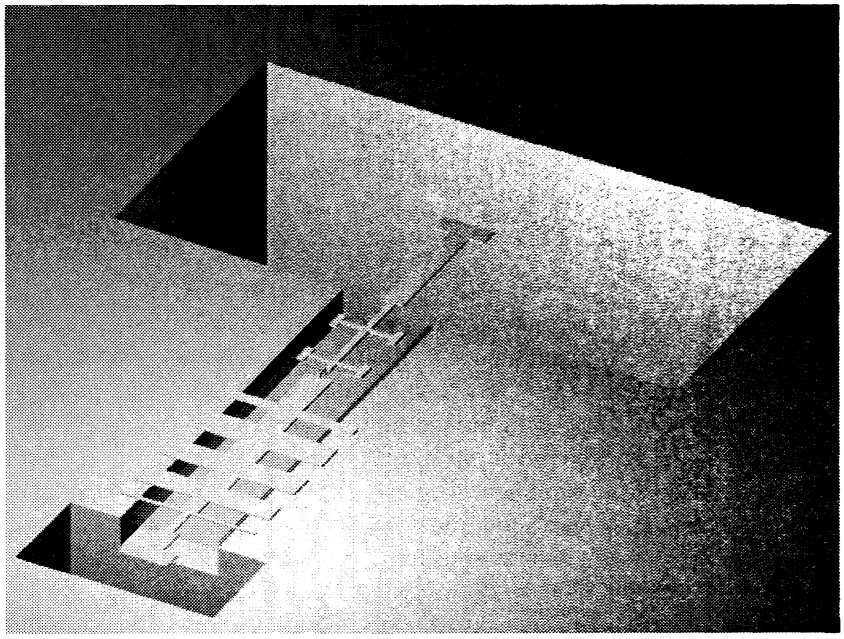

Figure 6. *A possible microstrip/waveguide realisation of a 500 GHz HBV quintupler.*

Figure 7 shows the simulated performance of an ideal element version of the quintupler circuit in Figure 6, when an OPT HBV is employed. The input power is 19 dBm at 100 GHz. The 3-dB bandwidth is approximately 5% and the conversion efficiency, as expected, 31%.

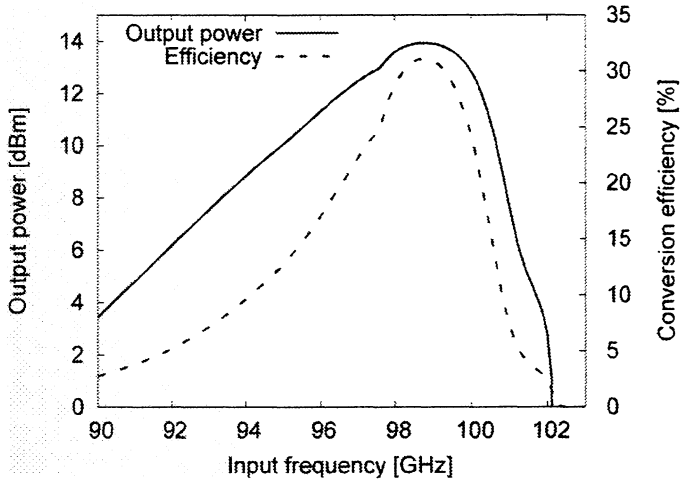

Figure 7. *Simulated output power and conversion efficiency for an ideal element version of the circuit in Figure 6. The input power is 19 dBm, and an OPT HBV is used.*

Conclusions

We have presented methods for the design and analysis of HBV frequency quintuplers with an output frequency of 500 GHz. HBVs were optimised using analytical, temperature dependent models. Optimum embedding impedances and estimated circuit performance were obtained from harmonic balance simulations in Microwave Office, for which HBV models have been developed. Finally, a possible microstrip/waveguide circuit realisation has been presented. An ideal element version of this circuit exhibits a maximum conversion efficiency of approximately 31% with a 3-dB bandwidth of 5%.

Acknowledgement

The authors would like to thank Professor Erik Kollberg for his continuous support and advice, and for being a great source of inspiration. This work is supported by the European Space Agency through the HBV Multiplier project, and the Swedish Foundation for Strategic Research, SSF.

References

[1] E. L. Kollberg and A. Rydberg, "Quantum-barrier-varactor diode for high efficiency millimeter-wave multipliers", *Electronics Letters*, vol. 25, pp. 1696-1697, 1989.

[2] J. Stake, L. Dillner, S. H. Jones, C. M. Mann, J. Thornton, J. R. Jones, W. L. Bishop and E. L. Kollberg, "Effects of Self-Heating on Planar Heterostructure Barrier Varactor Diodes", *IEEE Transactions on Electron Devices*, vol. 45, pp. 2298-2303, 1998.

[3] X. Mélique, A. Maestrini, E. Lheurette, P. Mounaix, M. Favreau, O. Vanbésien, M. Goutoule, G. Beaudin, T. Nähri and D. Lippens, "12% efficiency and 9.5 dBm output power from InP based heterostructure barrier varactor triplers at 250GHz", IEEE MTT-S International Microwave Symposium. Digest, Anaheim, pp. 123-126, 1999.

[4] J. Stake, S. H. Jones, L. Dillner S. Hollung and E. L. Kollberg, "Heterostructure Barrier Varactor Design", *IEEE Transactions on Microwave Theory and Techniques*, vol. 48, pp. 677-682, 2000.

[5] E. L. Kollberg, T. J. Tollmunen, M. A. Frerking and J. R. East, "Current Saturation in Submillimeter Wave Varactors", *IEEE Transactions on Microwave Theory and Techniques*, vol. 40, pp. 831-838, 1992.

[6] R. Williams, *Modern GaAs Processing Methods*, 2nd ed.: Artech House, 1990.

[7] M. Sotoodeh, A. H. Khalid, and A. A. Rezazadeh, "Empirical low-field mobility model for III-V compounds applicable in device simulation codes", *Journal of Applied Physics*, vol. 87, no. 6, pp. 2890-2900, 2000.

[8] B. Alderman, J.Stake, L. Dillner, D. P. Steenson, M. Ingvarson, E. Kollberg, C. Mann and J. Chamberlain, "A New Pillar Geometry for Heterostructure Barrier Varactor Diodes", Twelfth International Symposium on Space Terahertz Technology, 2001.

[9] E. L. Kollberg, J. Stake and L. Dillner, "Heterostructure barrier varactors at submillimetre waves", *Phil. Trans. R. Soc. Lond.* vol. 354, pp. 2383-2398, 1996.

[10] L. Dillner, J. Stake and E. L. Kollberg, "Modeling of the Heterostructure Barrier Varactor Diode", 1997 International Semiconductor Device Research Symposium, Charlottesville, pp. 179-182, 1997.

[11] Ø. Olsen, M. Ingvarson, and J. Stake, "A Low Cost Fixed Tuned F-band HBV Frequency Tripler," presented at IEEE MTT-S International Microwave Symposium, Philadelphia, 2003.